PAPER • OPEN ACCESS

Heart rate characteristic based modelling of atrial fibrillatory rate using implanted cardiac monitor data

View the article online for updates and enhancements.

Physiological Measurement
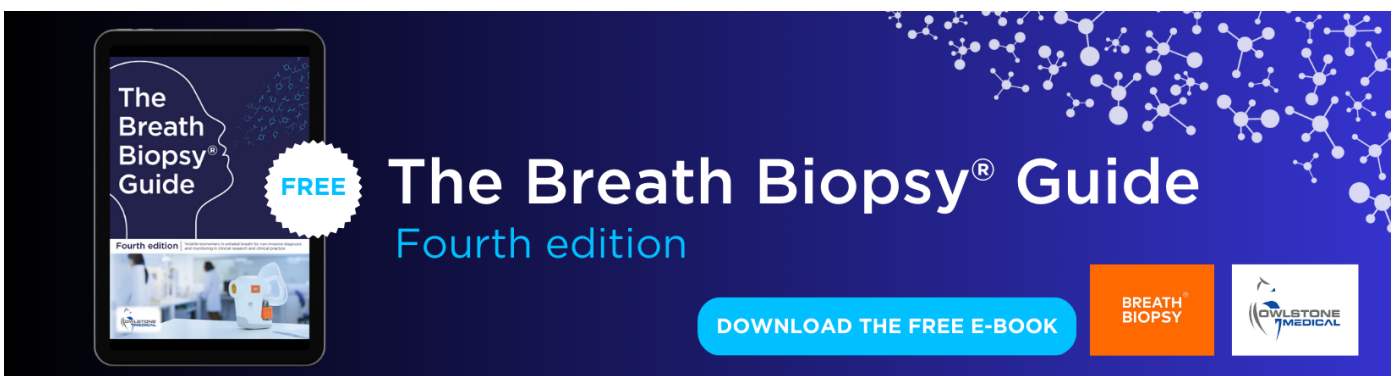
IPEM
Institute of Physics and
Engineering in Medicine

CrossMark

Heart rate characteristic based modelling of atrial fibrillatory rate using implanted cardiac monitor data

Javier Saiz-Vivo[1,2,*], **Mostafa Abdollahpur**[3], **Luca T Mainardi**[2], **Valentina D A Corino**[2,4], **Mirko De Melis**[1], **Robert Hatala**[5] **and Frida Sandberg**[3]

1 Medtronic: Bakken Research Center, Maastricht, The Netherlands
2 Department of Electronics, Information and Bioengineering, Politecnico di Milano, Milan, Italy
3 Department of Biomedical Engineering, Lund University, Lund, Sweden
4 Cardiotech Lab, Centro Cardiologico Monzino IRCCS, Milan, Italy
5 Department of Cardiology and Angiology, Division of Arrhythmias and Cardiac Pacing, National Institute of Cardiovascular Diseases and Slovak Medical University, Bratislava, Slovakia
* Author to whom any correspondence should be addressed.

E-mail: javier.saizvivo@medtronic.com

Abstract

Objective. The objective of the present study is to investigate the feasibility of using heart rate characteristics to estimate atrial fibrillatory rate (AFR) in a cohort of atrial fibrillation (AF) patients continuously monitored with an implantable cardiac monitor. We will use a mixed model approach to investigate population effect and patient specific effects of heart rate characteristics on AFR, and will correct for the effect of previous ablations, episode duration, and onset date and time. *Approach.* The f-wave signals, from which AFR is estimated, were extracted using a QRST cancellation process of the AF episodes in a cohort of 99 patients (67% male; 57 ± 12 years) monitored for 9.2(0.2–24.3) months as median(min-max). The AFR from 2453 f-wave signals included in the analysis was estimated using a model-based approach. The association between AFR and heart rate characteristics, prior ablations, and episode-related features were modelled using fixed-effect and mixed-effect modelling approaches. *Main results.* The mixed-effect models had a better fit to the data than fixed-effect models showing h.c. of determination ($R2 = 0.49$ versus $R2 = 0.04$) when relating the variations of AFR to the heart rate features. However, when correcting for the other factors, the mixed-effect model showed the best fit ($R2 = 0.04$). AFR was found to be significantly affected by previous catheter ablations ($p < 0.05$), episode duration ($p < 0.05$), and irregularity of the *RR* interval series ($p < 0.05$). *Significance.* Mixed-effect models are more suitable for AFR modelling. AFR was shown to be faster in episodes with longer duration, less organized *RR* intervals and after several ablation procedures.

1. Introduction

As the general population ages, the incidence of atrial fibrillation (AF) rises (Murray *et al* 2016). Nowadays, AF has become the most common arrhythmia encountered in clinical practices leading to increased mortality. However, the underlying mechanisms are still under investigation and appropriate patient selection for treatment still remains a challenge (Rottner *et al* 2020, Saglietto *et al* 2021). The opportunity to find additional ways of characterizing atrial electromechanical and anatomical properties and ways of predicting subsequent outcome after therapeutic intervention would favour timely therapy selection. More specifically, AF is related to a compromised atrial function caused by a fast and irregular atrial depolarization which can be characterized from the f-waves in the ECG. There have been many parameters introduced in the literature to characterize f-waves including their amplitude, frequency, morphology (Stridh and Sörnmo 2001, Corino *et al* 2007) and, atrial organization (Alcaraz and José 2007).

The f-wave frequency, often referred to as the atrial fibrillatory rate (AFR) is an AF characteristic which has been subject to considerable clinical attention. It has been shown to be a useful tool for monitoring drug effects (Platonov *et al* 2014) as well as for predicting outcomes from clinical procedures such as successful AF cardioversion (Bollmann *et al* 2003) and early AF recurrence (Bollmann *et al* 2008).

The correlation of AFR and several well-known HRV features describing the variability and irregularity of *RR* intervals during AF has been previously explored. While the analysis showed that variability parameters were independent from AFR, the irregularity parameters were significantly correlated with AFR (Corino *et al* 2013). However, the extrapolation of their findings for all clinical types of AF remains to be determined as the population used in the study included only patients with underlying congestive heart failure. In addition, the analysis did not account for variations on AFR due to circadian cycles, episode duration or previous ablations.

Circadian variations in the AF frequency within a 24 h period have been studied using Holter recordings in pursuit of understanding the underlying mechanisms of AF. It was concluded that AFR was significantly lower during night-time than during daytime (Bollmann *et al* 2000, Cosson *et al* 2000, Meurling *et al* 2001). These studies, however, have a drawback as AFR was computed from sparse measurements with several hours in between estimates. In addition, in one of the studies, two different sets of patients were identified: one which showed an increase (minority) while the other showed a decrease (majority) in nocturnal AFR (Bollmann *et al* 2000). A later study used more advanced signal processing techniques and obtained a more robust estiamates and a continuous AF frequency trend (Sandberg *et al* 2010). This study found that circadian variations were present in most of the patients with long-standing persistent AF analysed (13/18). However, the former and the latter studies have the drawback of having their insight on atrial electrophysiological characteristics during AF constrained to 24 h long Holter registrations, limited datasets of up to 30 patients and were all based on persistent and chronic AF patients.

Other studies have shown a positive correlation between episode duration and AFR ($R = 0.53$, $p < 0.05$) (Bollmann *et al* 1999). However, this study was conducted in a small dataset with only 31 episodes from 11 paroxysmal AF patients.

Implantable cardiac monitors (ICMs) with highly sensitive AF detection algorithms showing detection rates up to 96% (Hindricks *et al* 2010) are widely used in the clinical practice for the diagnosis and monitoring of AF. Clinical applications of these monitors include AF diagnosis after catheter ablation (Kapa *et al* 2013, Verma *et al* 2013) and cryptogenic stroke (Etgen *et al* 2013). These devices offer the advantage of long-term monitoring which can lead to a more detailed characterization of the AFR behaviour. These long monitoring periods spanning several months, thus including several episodes per patient, allow an analysis of the joint effects of HRV derived features and, circadian variation, episode duration and previous ablations on AFR.

The estimation of AFR from *RR* series data would enable wearable based assessment of AFR, e.g. wristband PPG, which would lead to a better characterization of the patient's condition. The aim of this study is to model variations in AFR using *RR* series features, by correcting for the effect of time of the day of episode onset, episode duration and previous ablations on AFR, in a cohort of AF patients continuously monitored with an ICM. The AFR was estimated using a model-based approach for f-wave analysis (section 2.2) that allowed for a robust estimation of AFR from ICM data. In a previous study regarding AFR and HRV, the analysis was conducted only on patients with underlying congestive heart failure and did not account for the presence of confounding factors (Corino *et al* 2013). We used a simple fixed-effect (FE) modelling approach using *RR* series features and compared it to two more complex mixed-effect (ME) modelling approaches: one to study both the population and patient specific effects of *RR* series in AFR and another that allowed correction for the effect of episode duration, previous ablations, and possible circadian variations. In addition, ME modelling will account for the heterogeneity within AF patients.

2. Materials and methods

2.1. Patient population

The present study population consisted of a subset of the cohorts of patients with symptomatic AF enrolled in the Reveal LINQ Usability study, a multi-centre single-arm clinical study (ClinicalTrials.gov Identifier: NCT01965899) (Sanders *et al* 2016), and a Slovak tertiary-care arrhythmia centre database (Bou Ezzeddine *et al* 2015). In both cohorts, the patients provided written informed consent, and the study protocols were reviewed and approved by the Human Research Ethics Committee of each participating institution in accordance with the Declaration of Helsinki. 99 patients (67% male, 33% female; 57 ± 12 years) had pre- and post-ablation monitoring and were included in the analysis. Nineteen patients had a previous failed ablation before the ablation procedure considered in this study. The clinical baseline characteristics of the analysed patients are shown in table 1.

Table 1. Baseline and clinical data of the study population ($n = 99$). PAF: Paroxysmal Atrial Fibrillation; CAD: Coronary Artery Disease.

	Patients ($n = 99$)
Age	57 ± 12
Male	66 (67%)
Female	33 (33%)
Coronary Risk Profile	
PAF	73 (74%)
Hypertension	40 (40%)
Diabetes	13 (13%)
CAD	5 (5%)
Stroke	3 (3%)
Previous Ablation	19 (19%)

The devices used in the Usability and the Slovakia studies were the Reveal LINQ and Reveal XT (Medtronic Inc., Minneapolis, MN), respectively which were implanted within the fourth intercostal space (V2-V3 electrode orientation) near the apex of the heart. The feasibility of extracting atrial activation from ICM data has been previously explored (Platonov *et al* 2012). Both devices record the signal with sampling frequency of 256 Hz and then sense and detect the rhythm by analysing *RR* interval patterns to compute an AF evidence score every 2 min. Due to memory restrictions, the devices store a single-lead ECG signal of 2 min of the AF episode detected as well as the ventricular sense, i.e. the positions of the R-peaks. In addition, the devices store the detected episode onset date and time, and the total duration of the episode.

The 99 patients included in the study had the ICM implanted and were followed-up for 9.2 (0.2–24.3) months as median (min-max). The ablation procedure was performed 5.8 (1.0–14.4) months after the implant. The ablation procedures were either pulmonary vein isolation (PVI) only (76 patients, 77%) or PVI plus extra lesions, which included roof and mitral lines, and ablation of complex fractionated atrial electrograms (23 patients, 23%). AF recurrence was defined as an AF episode detected by the ICM after a 3 month blanking period following catheter ablation and only those episodes outside the blanking period were considered in the analysis. The blanking period is based on reports describing how early recurrences could be caused by post-ablation inflammation or short-term autonomic imbalance rather than ablation failure (Hindricks *et al* 2021). In the analysed cohort, 31 (31%) had AF recurrence, 38 (38%) had no AF recurrence, and 30 patients (30%) left the study before the ending of the 3 months blanking period so there is no available information of their recurrence status. To evaluate the variations of AFR, the episodes occurring during the full monitoring period, except the 3 months blanking period, of the 99 patients included in the study were considered.

2.2. Estimation of AFR

The atrial activity, from which the AFR is computed, is extracted from ECG signals using Cardiolund ECG Parser (www.cardiolund.com).

Once the atrial activity ($x(n)$) having a length of N samples is obtained, a harmonic f-wave model (Henriksson *et al* 2018) is used to estimate the local f-wave frequency. In this model, the f-waves are modelled by a complex signal $s(n, \boldsymbol{\theta})$, defined as the sum of two harmonically related, complex exponentials with fundamental frequency f

$$s(n, \boldsymbol{\theta}) = \sum_{m=1}^{2} A_m e^{j\left(2\pi \frac{f}{f_s} mn + \phi_m\right)}, \tag{1}$$

$$\boldsymbol{\theta} = [f \ A_1 \ \phi_1 \ A_2 \ \phi_2]^T, \tag{2}$$

where A_m and ϕ_m define the amplitude and phase, respectively, of the m-th exponential (first and second), f_s is the sampling frequency and θ, the parameter vector.

The complex valued analytic representation $x_a(n)$ of the observed f-wave signal $x(n)$, is assumed to be composed of $s(n, \boldsymbol{\theta})$ and white, complex Gaussian noise e

$$\boldsymbol{x}_a(n) = \boldsymbol{s}(n, \boldsymbol{\theta}) + \boldsymbol{e} = \boldsymbol{Z}(\omega_0)\boldsymbol{a}(\boldsymbol{\theta}) + \boldsymbol{e}, \tag{3}$$
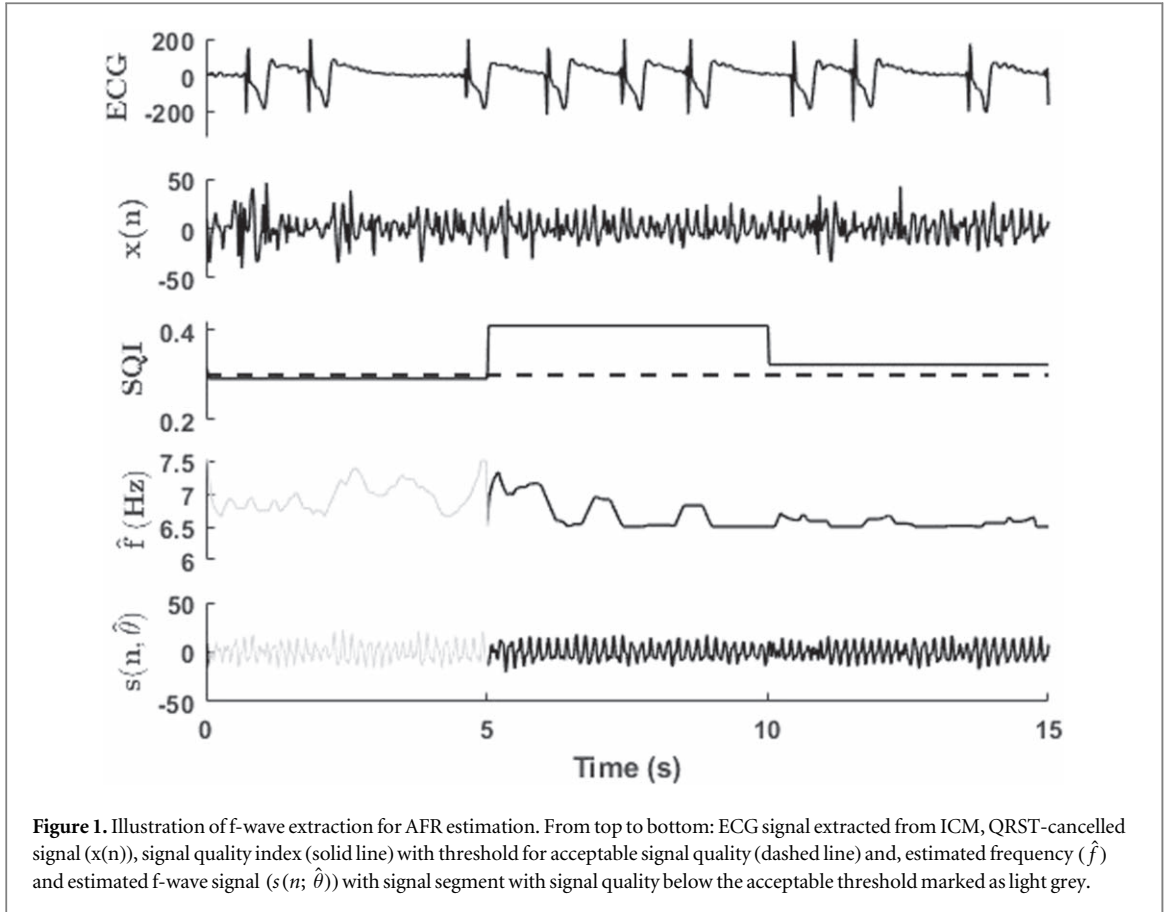
Figure 1. Illustration of f-wave extraction for AFR estimation. From top to bottom: ECG signal extracted from ICM, QRST-cancelled signal (x(n)), signal quality index (solid line) with threshold for acceptable signal quality (dashed line) and, estimated frequency ($\hat{f}$) and estimated f-wave signal ($s(n; \hat{\theta})$) with signal segment with signal quality below the acceptable threshold marked as light grey.

where $\omega_0 = 2\pi \frac{f}{f_s}$, $\boldsymbol{a}(\boldsymbol{\theta})$ is a 2×1 vector containing the amplitude and phase information:

$$\boldsymbol{a}(\boldsymbol{\theta}) = [A_1 e^{j\phi_1}\ A_2 e^{j\phi_2}]^T, \tag{4}$$

and $\boldsymbol{Z}(\omega_0)$ is an $N \times 2$ Vandermonde matrix defined as:

$$\boldsymbol{Z}(\omega_0) = \begin{bmatrix} 1 & 1 \\ e^{j\omega_0} & e^{j2\omega_0} \\ \vdots & \vdots \\ e^{j\omega_0(N-1)} & e^{j2\omega_0(N-1)} \end{bmatrix}. \tag{5}$$

The model is evaluated in 5 s windows by locally fitting the model in K 0.5 s overlapping sub-segments $x_{a,k}$, $k = 1,\ldots,K$ and estimating $\hat{\boldsymbol{\theta}}$ using a maximum likelihood approach. For each subsegment, the local frequency estimate $\hat{\omega}_{0,k}$ is determined by:

$$\hat{\omega}_{0,k} = arg\ min\ \|\boldsymbol{x}_{a,k} - \boldsymbol{Z}(\boldsymbol{Z}^H\boldsymbol{Z})^{-1}\boldsymbol{Z}^H\boldsymbol{x}_{a,k}\|^2, \tag{6}$$

where $Z \equiv Z(\omega_{0,k})$. The local frequency estimates are then averaged over the 5 s windows and the AFR of the segment is determined as:

$$\hat{f} = \sum_{k=1}^{K} \frac{\hat{\omega}_{0,k} f_s}{2\pi K}. \tag{7}$$

The model's fit is then evaluated using the model error $\hat{e}(n) = x_a(n) - s(n; \hat{\boldsymbol{\theta}})$ to estimate the signal quality index (SQI)

$$\text{SQI} = 1 - \frac{\sigma_{\hat{e}}}{\sigma_{x_a}}, \tag{8}$$

where $\sigma_{\hat{e}}$ and σ_{x_a} are the standard deviation of $\hat{e}(n)$ and $x_a(n)$. The SQI is confined between [0, 1] with larger values associated to a better fit. A fixed threshold is used to indicate whether f-waves have sufficient quality for the analysis. For this study, the SQI was estimated every 5 s windows and the threshold was set to 0.3 as suggested by Henriksson *et al* (2018). Figure 1 shows the f-wave extraction process for the AFR estimation.

For further details on the estimation of AFR and the SQI, the reader is referred to Henriksson *et al* (2018).

For each episode, the local f-wave frequency calculated for each 5 s segment is then averaged over the estimates of sufficient signal quality, thus obtaining the AFR.

The mean AFR of at least one acceptable 5 s segment was considered to be representative of the first minutes of the AF episode under the assumption that the AFR was stable within 2 min of AF. The stability of AFR within the episodes was studied by selecting the episodes where more than 80% of the episode had acceptable levels of SQI and iteratively computing the mean AFR for decreasing percentages of the signal. In each iteration, an additional random 5 s segment was left out and the relative absolute error between the mean AFR of the reduced signal segments and the mean AFR of the whole acceptable signal was evaluated.

2.3. Modelling

FE models are statistical models which only contain fixed effects. In contrast, ME models contain both fixed effects and random effects, and are useful when dealing with data involving multiple sources of random error such as repeated measures within subjects (Stroup 2013).

In general terms, for the ME model in this analysis, we consider N patients, with the index i representing the ith patient ($1 \leqslant i \leqslant N$). Each patient has n_i measurements y_{ij}, with the index j representing the jth episode ($1 \leqslant j \leqslant n_i$). P then is defined as the total number of episodes included in the analysis so that $P = \sum_1^N n_i$. There are M random effects considered, and the patient-specific random effect is represented by b_{im} ($1 \leqslant m \leqslant M$). The y_{ij} of each episode j in each patient i is assumed to follow a Gaussian distribution:

$$(y_{ij}|b_{0i}, b_{1i}, \ldots b_{Mi}) \sim N(\mu_{ij}| b_{0i}, b_{1i}, \ldots b_{Mi}, \sigma^2), \tag{9}$$

where $\mu_{ij}|b_{0i}, b_{1i}, \ldots b_{Mi}$ is the conditional expectation of the observations, in this case the AFR of each episode y_{ij}, given by random vector $\boldsymbol{b_i}$, containing the patient specific random effects $[b_{0i}, b_{1i}, \ldots b_{Mi}]$, and σ^2 is the dispersion parameter of the distribution.

Linear ME models can be represented as:

$$\boldsymbol{y} = \boldsymbol{X\beta} + \boldsymbol{Zb} + \boldsymbol{e}, \tag{10}$$

where $\boldsymbol{y}$ is the set of y_{ij}, $\boldsymbol{X}$ is the design matrix for fixed effects, i.e. not dependent on the patient, $\boldsymbol{Z}$ is the design matrix for random effects, $\boldsymbol{\beta}$ is a vector of fixed effect parameters $[\beta_0, \beta_1, \ldots, \beta_M]$, $\mathbf{b}$ contains the N sets of $\boldsymbol{b_i}$, and $\boldsymbol{e}$ contains the random errors associated with the ijth observation. The design matrix $\boldsymbol{X}$ ($P \times M + 1$) is defined by:

$$\boldsymbol{X} = [\boldsymbol{x}_{\beta_0} \boldsymbol{x}_{\beta_1} \boldsymbol{x}_{\beta_2} \ldots \boldsymbol{x}_{\beta_M}], \tag{11}$$

where $\boldsymbol{x}_{\beta_0}$ is a $P \times 1$ binary vector for patient independent intercept β_0, and $[\boldsymbol{x}_{\beta_1}, \boldsymbol{x}_{\beta_2}, \ldots, \boldsymbol{x}_{\beta_M}]$ is a $P \times M$ matrix which contains the values for each of the M features describing the episodes considered in the analysis. Similarly, the design matrix for the random effects $\boldsymbol{Z}$ ($P \times N_* (M + 1)$) is defined by:

$$\boldsymbol{Z} = [\boldsymbol{Z}_{\boldsymbol{b}_0} \boldsymbol{Z}_{\boldsymbol{b}_1} \boldsymbol{Z}_{\boldsymbol{b}_2} \ldots \boldsymbol{Z}_{\boldsymbol{b}_M}], \tag{12}$$

where $\boldsymbol{Z}_{\boldsymbol{b}_0}$ is the $P \times N$ binary matrix for $\boldsymbol{b}_0$, the patient specific intercept vector containing $[b_{01}, b_{02}, \ldots, b_{0N}]$ intercepts, and $[\boldsymbol{Z}_{\boldsymbol{b}_1} \boldsymbol{Z}_{\boldsymbol{b}_2} \ldots \boldsymbol{Z}_{\boldsymbol{b}_M}]$ contains the values z_{bm}^{ij} which represent the value of feature m describing the jth episode of the ith patient.

The maximum pseudo likelihood method is employed for the parameter estimation. For ME models with observations $\boldsymbol{y}|\boldsymbol{b} \sim N(\boldsymbol{\mu}|\boldsymbol{b}, \boldsymbol{R})$ with $\boldsymbol{b} \sim N(0, \boldsymbol{G})$, being $\boldsymbol{R}$ and $\boldsymbol{G}$, variance matrices for distributions of $\boldsymbol{y}|\boldsymbol{b}$ and $\boldsymbol{b}$ respectively, the log-likelihood equation can be written as (Stroup 2013):

$$\ln \mathcal{L}(\boldsymbol{y}, \boldsymbol{b}) = -\left(\frac{1}{2}\right)(\boldsymbol{y} - \boldsymbol{X\beta} - \boldsymbol{Zb})'\boldsymbol{R}^{-1}(\boldsymbol{y} - \boldsymbol{X\beta} - \boldsymbol{Zb}) - \left(\frac{1}{2}\right)\boldsymbol{b}'\boldsymbol{G}^{-1}\boldsymbol{b}. \tag{13}$$

The estimator is then given by:

$$(\hat{\boldsymbol{y}}, \hat{\boldsymbol{b}}) = \underset{(\boldsymbol{y}, \boldsymbol{b})}{arg\max}(\ln \mathcal{L}(\boldsymbol{y}, \boldsymbol{b})); \tag{14}$$

see (Stroup 2013) for details on the maximum pseudo likelihood method.

FE models can be represented as in equation (10) but with the random effects coefficient $\mathbf{b}$ being equal to 0. Hence, the log-likelihood equation can be written as:

$$\ln \mathcal{L}(\boldsymbol{y}) = -\left(\frac{1}{2}\right)(\boldsymbol{y} - \boldsymbol{X\beta})'\boldsymbol{R}^{-1}(\boldsymbol{y} - \boldsymbol{X\beta}), \tag{15}$$

and the estimator is given by:

$$(\hat{\boldsymbol{y}}) = \underset{(\boldsymbol{y})}{arg\max}(\ln \mathcal{L}(\boldsymbol{y})); \tag{16}$$

In this study, a linear FE model is used to evaluate the effects of changes in *RR* series characteristics on AFR. In addition, the results obtained will be compared to two ME models which will evaluate both the fixed and random effects of circadian variations, previous ablations, episode duration and *RR* series characteristics on AFR.

Following the previous formulations, y_{ij} corresponds to the AFR_{ij} of the ijth episode, $\mathbf{X}$ and $\mathbf{Z}$ contain the features comprised by time, number of ablations, duration of episode and heart rate characteristic features, and $\boldsymbol{\beta}$ and $\boldsymbol{b}$ contain the fixed and random effects of the model.

The FE and ME models (described bellow) were fitted and evaluated using Matlab R2022a (The Mathworks Inc., Natick, Massachusetts). The Akaike Information Criterion (AIC) (Akaike 1974) and the deviance residual, i.e. an index of model fit, where a model with a higher deviance provides a poorer model fit to the data than a model with a lower deviance (Zeng *et al* 2014), are used to select the model which fits best the dataset. In addition, to check the goodness of fit of the models, the fitted values of AFR are compared to the observed values of AFR, and the coefficients of determination (R^2) (Wright 1921) are computed.

2.3.1. Fixed-effect model of AFR

From the ventricular sense of the AF episode stored in the ICM, heart rate characteristic features are computed to represent the variability and irregularity of the RR intervals in each episode. For this study, the parameters extracted were the mean RR intervals (mean interval between ventricular senses in milliseconds), the mean squared differences of successive RR intervals (RMSSD) expressed in milliseconds and calculated as:

$$\text{RMSSD} = \sqrt{\frac{\sum_{i=1}^{N-1}(RR_{i+1} - RR_i)^2}{N-1}}, \tag{17}$$

where RR_i is the ith RR interval, RR_{i+1} the successive interval, and N is the total number of RR intervals, and the sample entropy (SampEn). SampEn estimates the irregularity of the RR series and was computed as described in (Richman and Moorman 2000). To compute SampEn, the length of the vectors to be compared in the calculation (m) and the noise rejection level (r) must be selected. In this study, the chosen parameters were $m = 2$ and $r = 0.2\sigma$, where σ is the standard deviation of the RR intervals.

The **FE model** assumes fixed (population) effects of RR mean, RR variability and RR irregularity on AFR (Mean RR, RMSSD and SampEn) hence an estimate of AFR ($\hat{AFR}_{ij}$), for patient i and episode j, is given by:

$$\hat{AFR}_{ij} = \beta_0 + \beta_1 \times MeanRR_{ij} + \beta_2 \times RMSSD_{ij} + \beta_3 \times SampEn_{ij}, \tag{18}$$

where β_0 is the intercept estimate for the fixed effect. In a similar way, β_1, β_2 and β_3 represent the fixed effects of the Mean RR, RMSSD and SampEn respectively, in Model *FE*.

2.3.2. Mixed-effect model of AFR

In order to account for the heterogeneity between patients, an ME model is used. The **ME model** assumes both the fixed and random effects of changes in RR series on AFR by introducing the patient-specific random effects to equation (18):

$$\hat{AFR}_{ij} = \beta_0 + b_{0i} + (\beta_1 + b_{1i}) \times MeanRR_{ij} + (\beta_2 + b_{2i}) \times RMSSD_{ij} + (\beta_3 + b_{3i}) \times SampEn_{ij}, \tag{19}$$

where b_{0i} represents the intercept estimate for the patient-specific random effect, and b_{1i}, b_{2i} and b_{3i} represent the patient-specific random effect of Mean RR, RMSSD and SampEn respectively.

2.3.3. Mixed-effect model of AFR and correct for confounding factors

There are several variables that could affect AFR and need to be accounted for. In this study, the effect of circadian variations quantified by the episode onset time, the effect of multiple ablations, the effect of the long monitoring periods quantified by the time since ICM implant, and the effect of episode duration will be used to correct the *ME* model.

The circadian variations of AFR were modelled by considering the time of the day of the onset of each AF episode. In order to relate AFR with circadian variation which has a cyclical nature, the time onset parameter was transformed into a sinusoid where -1 represents the middle of the day (12:00) and 1 represents the middle of the night (00:00) using the following expression:

$$\text{Time} = \cos\left(2\pi\frac{\text{Time}_{24h}}{24}\right), \tag{20}$$

where Time_{24h} represents the 24 h based AF onset and Time the modified AF onset used in the analysis.

Furthermore, the patients of this cohort have undergone one or two ablation procedures in their lifetimes. The '*nAblations*' parameter represents the number of ablations undergone by the patient at the time of the episode onset. This parameter can either be 0 for patients with no previous ablations in episodes occurring before their first ablation, 1 for patients after their first ablation or before their second ablation, or 2 for patients with a previously failed ablation and after their second ablation. This parameter will correct for the effect on AFR of episodes occurring pre- and post-ablation as well as for patients with previously failed ablation procedures with compromised atria.

In addition, the patients of this cohort have been followed up for long monitoring periods, so the feature *'DaysSinceImplant'* represents the period between the episode onset date and the date the patients were implanted with the ICM. This parameter will correct for the effects of the long monitoring periods on AFR; the change in DaysSinceImplant provides a common timescale for the episodes included in the analysis.

Lastly, in addition to the onset time and date, the Reveal LINQ also stores the total duration of the episode in minutes, i.e. *'Duration'*.

The complete ***ME*'** **model** assumes the fixed and random effects of changes in the *RR* series, and corrects for circadian variation, number of ablations and episode duration:

$$A\hat{F}R_{ij} = \beta'_0 + b'_{0i} + (\beta'_1 + b'_{1i}) \times MeanRR_{ij} + (\beta'_2 + b'_{2i}) \times RMSSD_{ij} + (\beta'_3 + b'_{3i}) \times SampEn_{ij} + (\beta'_4 + b'_{4i}) \times \text{Time}_{ij}$$
$$+ (\beta'_5 + b'_{5i}) \times nAblations_{ij} + (\beta'_6 + b'_{6i}) \times DaysSinceImplant_{ij} + (\beta'_7 + b'_{7i}) \times \text{Duration}_{ij},$$

$$(21)$$

where β'_4, β'_5, β'_6 and β'_7 represent the fixed effects of the circadian variations, number of ablations, period between implant date and onset and episode duration respectively, and b'_{4i}, b'_{5i}, b'_{6i} and b'_{7i} represent the patient-specific random effects. β'_0, b'_{0i}, β'_1, b'_{1i}, β'_2, b'_{2i}, β'_3 and b'_{3i} correspond to the fixed and patient-specific random effects introduced in equations (18) and (19) but for the ME' model.

2.4. Model evaluation

To evaluate the model's performance with unseen data, the episodes are partitioned into training and test sets. As the ME and ME' models are patient-specific, the training set was comprised of the earliest 80% of the episodes from each patient while the test set was comprised of the latest 20% of the episodes.

For comparison the FE model, that is patient-independent, was also evaluated using a training set comprised of the episodes from 80% of the patients and a test set comprised of the episodes from the remaining 20% patients.

In both cases, the accuracy was defined as the proportion of episodes where the estimated AFR deviated less than a certain absolute value from the true AFR.

2.5. Statistical analysis

Continuous data are presented as mean $\pm$ standard deviation if the null hypothesis H_0 of the Kolmogorov–Smirnov test (H_0: data is normally distributed) was not rejected. Otherwise, continuous data are presented as median (min-max). Categorical data are presented as absolute frequency (relative frequency in percentage). The null hypothesis was rejected when $p < 0.05$, then set as the level of significance. The relationship between the features was studied using the patient-average of the features and Pearson's linear pair-wise correlation between them was evaluated. This average was defined for each patient as the mean feature extracted from their episodes for those normally distributed features (such as *AFR*, *MeanRR* and *SampEn*) and the median feature extracted from their episodes for those not normally distributed features (such as Time and Duration). The normality of the feature was determined by analysing the complete set of episodes. In addition, to study the multicollinearity among features, Belsley's collinearity test was performed on the complete set of episodes. To check for collinearity, the number of near dependencies was first determined as the number of dependencies with conditional index (η_p) for p dependencies over the threshold $\eta^* = 30$. The features will be considered to have collinearity if their variance-decomposition proportion within the near dependencies exceeds the threshold $\pi^* = 0.5$ as suggested in Belsley (1991).

The statistical analysis was performed using Matlab R2022a (The Mathworks Inc., Natick, Massachusetts).
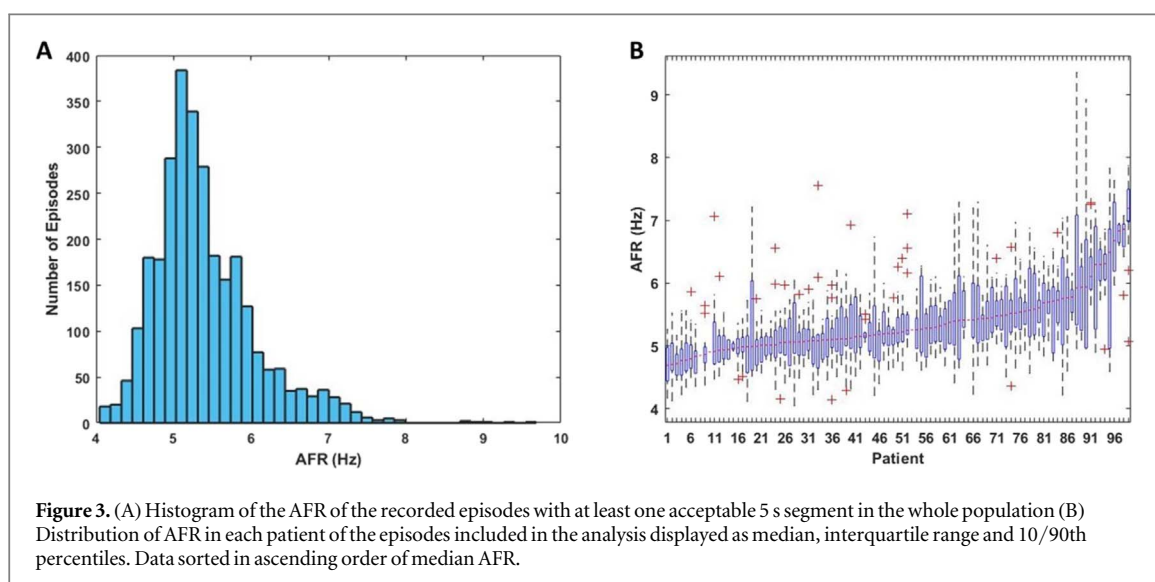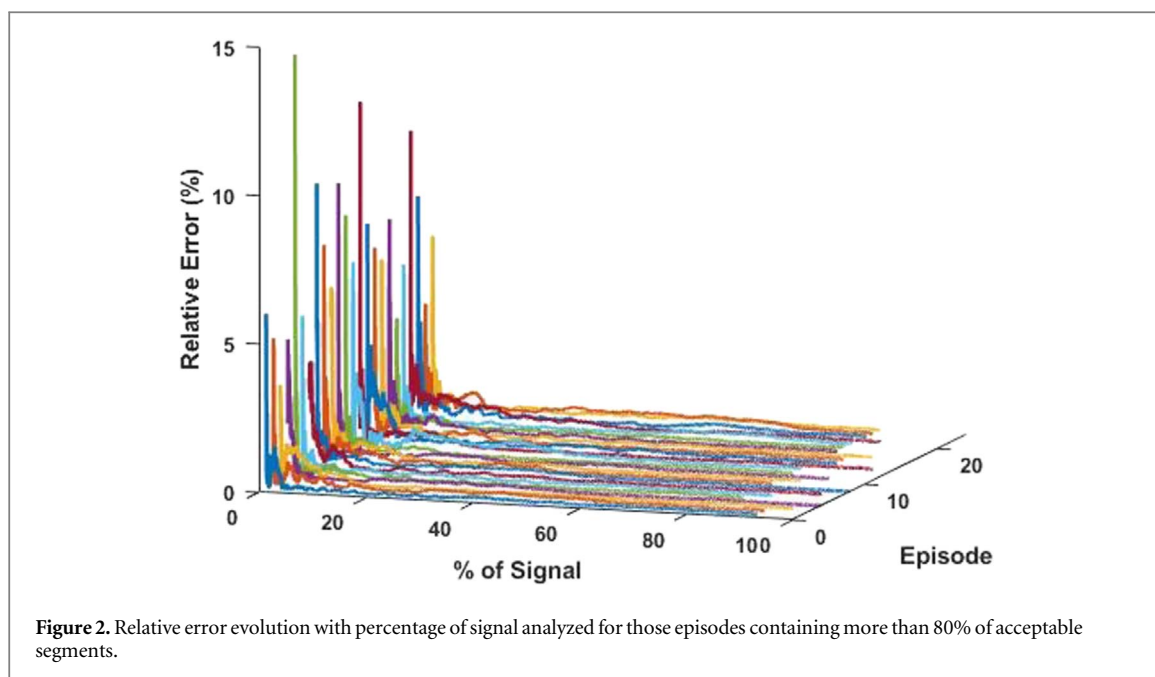
3. Results

During the monitoring period, the ICMs stored 3739 episodes out of which 2908 (77%) episodes contained at least one 5 s segment of sufficient signal quality for estimation of AFR. Only one segment of sufficient signal quality was required as AFR was assumed to be stable during the first 2 min of the AF episode. The stability analysis showed a maximum relative error of 7.2 (4.4)% for the 24 episodes where more than 80% of the episode had acceptable levels of SQI. Figure 2 shows the evolution of the relative error (%) for varying percentages of signal.

Out of the 2908 included in the analysis, 1796 (62%) occurred before ablation, 657 (23%) occurred after ablation and 455 (15%) occurred during the 3 months blanking period and were excluded from the analysis.

Each patient had a median (min-max) of 20.5 (2–114) episodes with 16 (0–77) episodes pre-ablation, and for the patients with AF recurrence, 10 (1–61) episodes post-ablation.

Figure 3(A) shows the histogram of the AFR extracted from the episodes with at least one acceptable 5 s segment in the whole population and (B) the distribution of AFR for each patient.

Figure 2. Relative error evolution with percentage of signal analyzed for those episodes containing more than 80% of acceptable segments.

Figure 3. (A) Histogram of the AFR of the recorded episodes with at least one acceptable 5 s segment in the whole population (B) Distribution of AFR in each patient of the episodes included in the analysis displayed as median, interquartile range and 10/90th percentiles. Data sorted in ascending order of median AFR.

The full dataset of AF episodes has a median AFR (min-max) of 5.3 (4.0 − 9.7) Hz. A high proportion (85%) of the AFR extracted from the episodes considered in the analysis were comprised between 4 and 6 Hz. A considerable variation in AFR between episodes is observed for some patients, whereas AFR remains similar between episodes for others.

The scatter plots of the patient-average AFR, modified time of AF onset, duration of AF episode (in log scale), and Mean *RR*, RMSSD and SampEn are shown in figure 4.

The patient-average AFR shows a mild significant linear correlation with the patient-average SampEn ($R = 0.27$, $p < 0.05$). Regarding the three HR characteristic features, the patient-average mean *RR* interval had a strong correlation with patient-average RMSSD ($R = 0.677$, $p < 0.001$) and a mild correlation with patient-average SampEn ($R = 0.312$, $p < 0.05$). The patient-average time also shows a mild correlation with the partient-average mean *RR* interval ($R = 0.203$, $p < 0.05$). In addition, the frequency distribution histograms of the patient-averages of the features studied are also aligned diagonally on the subpanels of figure 4. This frequency distribution histograms show that the average AF episode duration for each patient is predominantly short episodes with 54 patients (55%) having an average episode duration shorter than 20 min. Overall, the duration of the episodes had a median of 14 min with the minimum duration being the detection threshold, i.e. 2 min, and the maximum duration spanning 62.7 d.
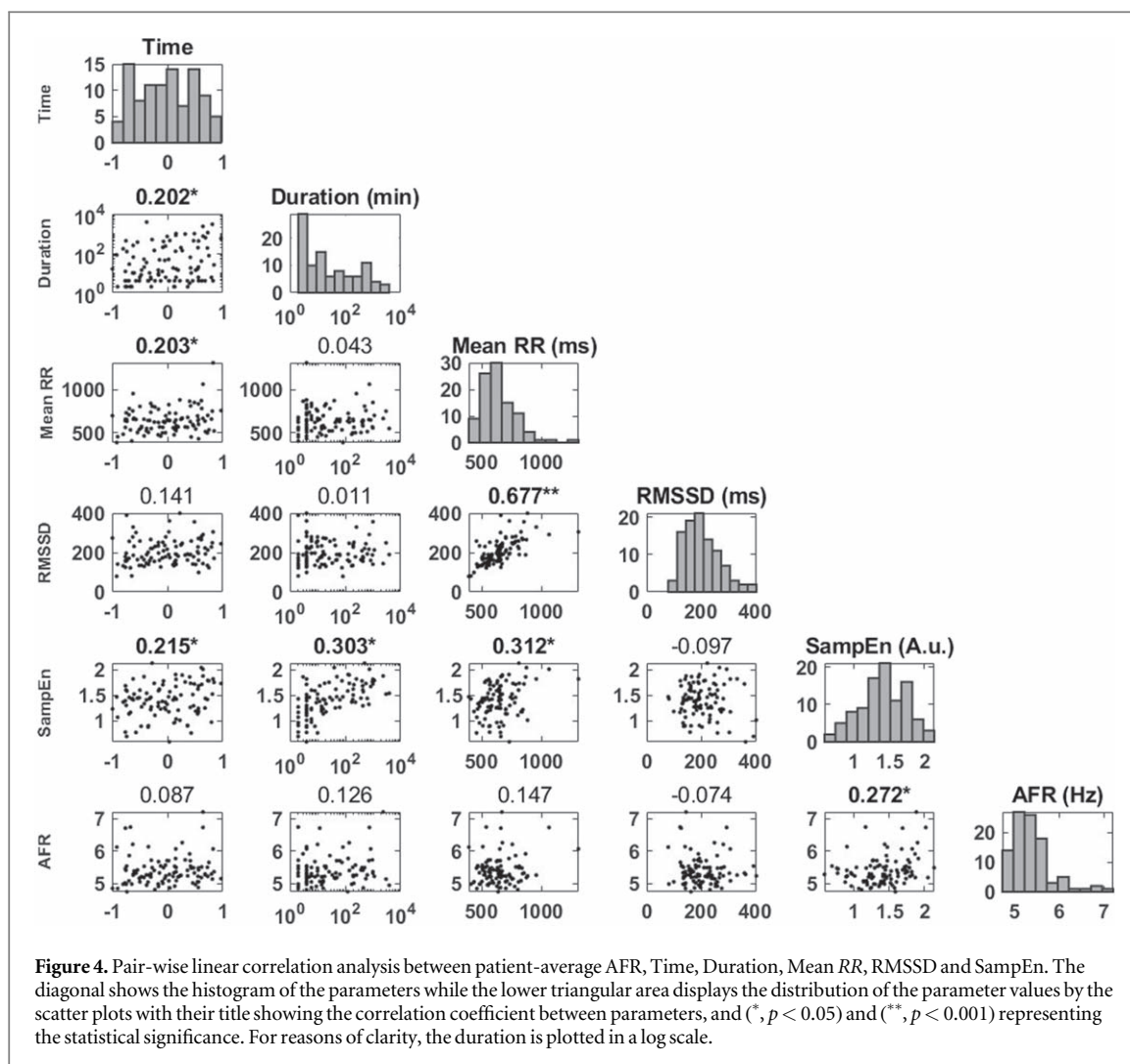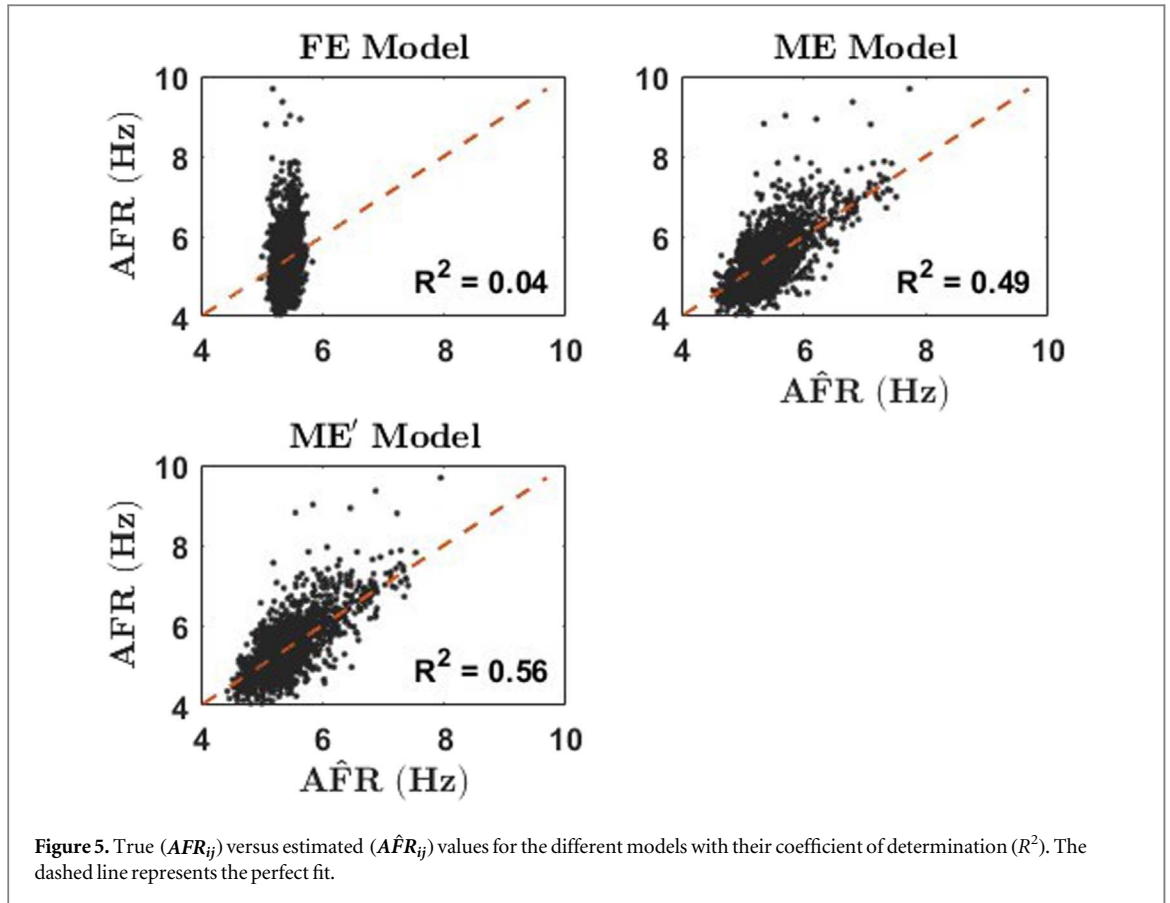
Figure 4. Pair-wise linear correlation analysis between patient-average AFR, Time, Duration, Mean *RR*, RMSSD and SampEn. The diagonal shows the histogram of the parameters while the lower triangular area displays the distribution of the parameter values by the scatter plots with their title showing the correlation coefficient between parameters, and (*, $p < 0.05$) and (**, $p < 0.001$) representing the statistical significance. For reasons of clarity, the duration is plotted in a log scale.

Table 2. Results comparison between the different models; AIC: Akaike Information Criterion; R^2: coefficient of determination; FE: Fixed-effect model; ME: Mixed-effect model, ME′: Complete ME model.

Model	Input variable	AIC	deviance	R^2
FE	Mean *RR* RMSSD SampEn	5699	5689	0.04
ME	Mean *RR* RMSSD SampEn	4424	4394	0.49
ME′	Mean *RR* RMSSD SampEn Time nAblations DaysSinceImplant Duration	4298	4208	0.56

The Belsley's collinearity test shows that the scaled condition indeces η_p are [1.00, 2.06, 2.15, 2.18, 3.26, 5.23, 9.59, 14.7] which are all bellow the defined threshold $\eta^* = 30$. Therefore, the dataset exhibits no multicollinearity.

Figure 5. True (AFR_{ij}) versus estimated ($A\hat{F}R_{ij}$) values for the different models with their coefficient of determination (R^2). The dashed line represents the perfect fit.

The results of the different models are summarized in table 2, and the fitted values of AFR were plotted against the true values and illustrated in figure 5.

The FE model, which only included the fixed effect of changes in *RR* series had the lowest complexity but had also the largest AIC value. When also considering the random effects in the ME model, the values of AIC and the deviance decreased. Lastly, when accounting for the circadian variation, the duration of the episode, the number of ablations before the episode and correcting for the monitoring period as in the ME′ model, the deviance and AIC value is minimum. This suggests that the ME′ model outweighs the other models also when accounting for the increased model complexity. The coefficients of determination (R^2) also corroborate that the ME′ model has the better fit as its coefficient is the highest ($R^2 = 0.56$).

The patient-wise root mean square error (RMSE) was computed for the ME' model and a median (min-max) RMSE of 0.35 (0.04–1.19) was found. This shows that for a subset of patients, the model is capable of estimating the AFR. In contrast, the other models had a patient-wise RMSE of 0.55 (0.24–1.74) in the case of the fixed model (FE) and 0.43 (0.02–1.39) when introducing the random effects (ME), which indicate a worse fit to the data. In addition, the Bland-Altman test (Altman and Bland 1983) is illustrated in figure 6, from which the limits of agreement can be seen to lie between 0.82 and −0.82 Hz (mean difference of 0 Hz and standard deviation of 0.42 Hz).

The estimation and the results for the fixed effect coefficients for the ME′ model are summarized in table 3.

The parameter associated to the intercept ($\beta'_0 = 4.979$, p < 0.001) is comparable to the average AFR, see figures 3 and 4.

The irregularity in *RR* intervals has a significant effect on the AFR ($\beta'_3 = 0.105, p < 0.05$) with higher AFR for higher irregularity. The number of prior ablations also has a significant effect on the AFR ($\beta'_5 = 0.168$, $p < 0.05$) with higher AFR after multiple ablations, and so does the episode duration ($\beta'_7 = 1.182 \times 10^{-5}, p < 0.05$) with AFR being higher for longer episodes.

The models performance in unseen data, evaluated as described in section 2.4, is illustrated in figure 7. In (A), the training set consists of the first 80% of episodes for each patient and the test set consist of the remaining 20% of the episodes. From the available 2884 episodes, 2346 (81.3%) were included in the training set and the remaining 538 (18.7%) were included in the test set. The accuracy of the models was then computed for varying absolute differences between the estimated AFR and the true AFR. As before, the results show that ME models fit the training set better than the FE model. However, both models overfit the data and the accuracies for the test set are lower with fewer than 50% of the estimated episodes within ±0.3 Hz of the true AFR.
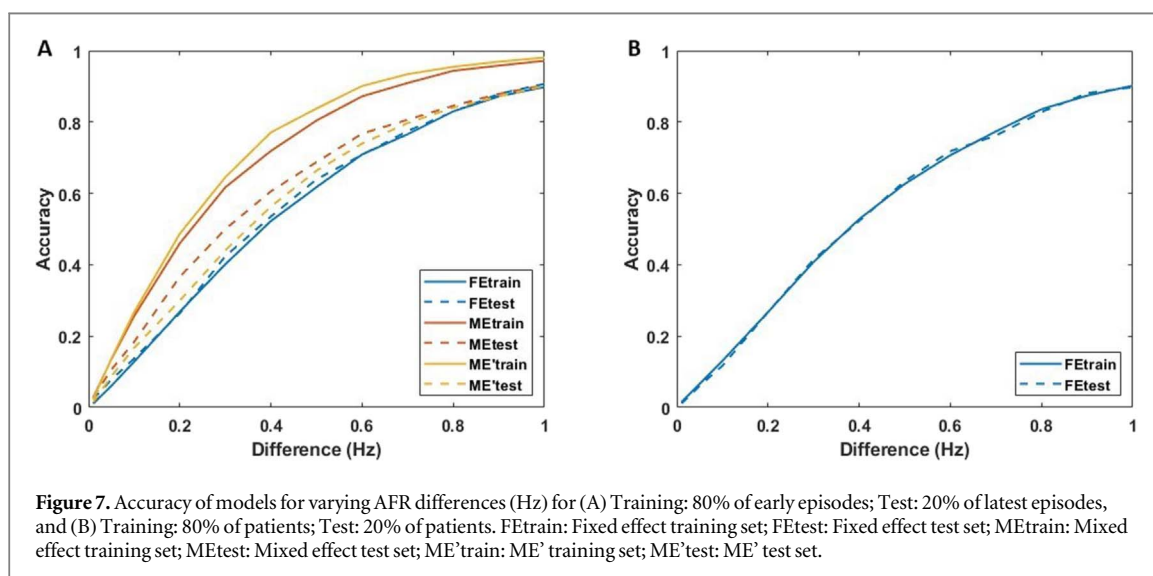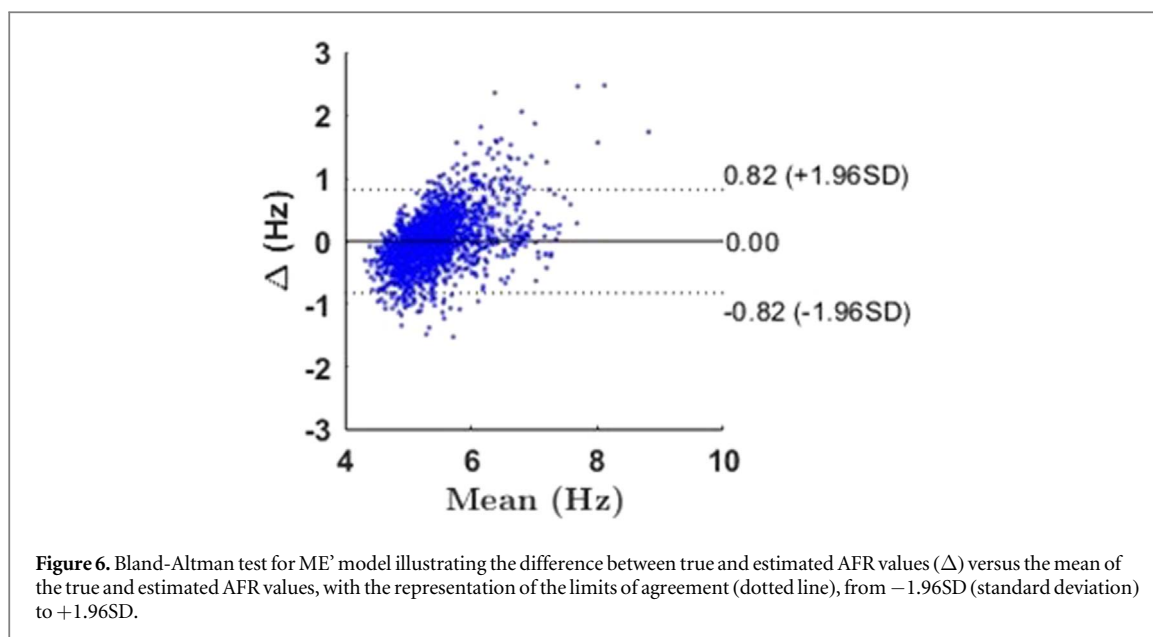
Figure 6. Bland-Altman test for ME' model illustrating the difference between true and estimated AFR values (Δ) versus the mean of the true and estimated AFR values, with the representation of the limits of agreement (dotted line), from -1.96SD (standard deviation) to $+1.96$SD.

Figure 7. Accuracy of models for varying AFR differences (Hz) for (A) Training: 80% of early episodes; Test: 20% of latest episodes, and (B) Training: 80% of patients; Test: 20% of patients. FEtrain: Fixed effect training set; FEtest: Fixed effect test set; MEtrain: Mixed effect training set; MEtest: Mixed effect test set; ME'train: ME' training set; ME'test: ME' test set.

Table 3. Fixed effect coefficients for the ME' model. (*, $p < 0.05$) and (**, $p < 0.001$) representing statistical significance. SE: Standard Error of the estimate.

Parameter	Associated to:	Estimate	SE	*p*-value
β'_0	Intercept	4.979	0.100	$<0.001^{**}$
β'_1	Mean *RR*	8.853×10^{-5}	2.289×10^{-4}	0.698
β'_2	RMSSD	5.453×10^{-4}	4.040×10^{-4}	0.177
β'_3	SampEn	0.105	0.047	0.031^*
β'_4	Time	-0.021	0.034	0.521
β'_5	Number of Ablations	0.168	0.073	0.022^*
β'_6	Days Since Implant	-5.323×10^{-5}	2.440×10^{-4}	0.827
β'_7	Duration	1.182×10^{-5}	3.721×10^{-6}	0.002^*

In (B), the patients were divided into training and test sets. As FE models do not rely on patient-specific estimates, the episodes of these patients were stratified into one of the two sets. From the available 98 patients, 78 (79.5%) were selected for the training set including 2349 episodes and the remaining 20 (20.5%) were selected for the test set including 547 episodes. In this case the accuracy of the training set and the test set were similar, however, the accuracy of both is relatively low.

4. Discussion

The rapidly increasing use of continuous monitoring devices for patients diagnosed with AF (Lee and Mittal 2018) offers the chance of a more detailed characterization and a better understanding of the patients' condition in order to select the most appropriate therapy but above all, the right timing in order to avoid disease deterioration. Continuous assessment of AFR extracted from ECG strips is a non-trivial matter. However, the estimation of AFR from *RR* series data would enable wearable based assessment of AFR, e.g. wristband PPG. The aim of the study was to model variations in AFR based on changes of *RR* series characteristics (mean *RR* interval, RMSSD and sample entropy). After a first attempt using FE modelling approach (FE model), the results were compared to more complex ME modelling approaches: considering both population and specific effects of *RR* series (ME model) and allowing correction for the effect of episode duration, previous ablations, and possible circadian variations (ME′ model). In addition, ME modelling would account for the heterogeneity within AF patients. In order to apply the different models, the AFR stability within 2 min of AF episodes was evaluated. In the 24 episodes with enough data to run the analysis we found that for different percentages of signal, the error between the mean AFR of the signal and the mean AFR on the remaining segments was 7.2 (4.4)%. With this result in mind, AFR was considered stable and the mean AFR calculated on a single segment (5 s) was considered representative of the whole signal.

We conclude from this initial analysis that there are no strong linear correlations between AFR and *RR* series characteristics in the present dataset and that the relationship between *RR* characteristics and AFR is more complex. It should be noted that the aim of the present study is to investigate the feasibility of estimating AFR from *RR* series data and not to develop an AFR estimator. The small size of the present dataset prevents us from using more complex modelling approaches due to the risk of overfitting. In the study of the multicollinearity among the variables, the dataset exhibited no multicollinearity in the Belsley's collinearity test. In addition, when evaluating the model performance with unseen data, the results show that while the ME models are able to fit the data better than the FE model, they overfit the data and produce low accuracies in the test set. This points out the difficulties and unreliability of estimating AFR using such simple regression models such as ME or FE and calls for further investigation with larger datasets and more complex models to be able to reach clinically acceptable accuracies.

The correlation between AFR and HRV features describing the variability and irregularity of *RR* intervals has been explored before in a cohort of patients with underlying congestive heart failure (Corino *et al* 2013). However, to the best of our knowledge, this is the first study to assess the variation of AFR in AF patients without congestive heart failure which were continuously monitored over several months. It is also the first study to model AFR variations using ME models which account for the heterogeneity of the patient population and confounding factors.

The model's parameters showed a significant effect of *RR* irregularity quantified by SampEn ($\beta'_3 = 0.105$, $p < 0.05$), number of ablations ($\beta'_5 = 0.168$, $p < 0.05$), and episode duration ($\beta'_7 = 1.182 \times 10^{-5}$, $p < 0.05$) on AFR. Due to the heterogeneity between patients, the ME model developed with correction for the confounding factors (ME′ model) was able to better fit the data compared to the FE model, the FE modelling approach, ($R^2 = 0.56$ versus $R^2 = 0.04$).

The fact that average SampEn is correlated with average AFR ($R = 0.27$, $p < 0.05$) and that it has a significant effect on AFR when evaluating the ME′ model, is in line with a previous study (Corino *et al* 2013) which evaluated the relationship between AFR and HRV derived features. In the aforementioned study, the regularity statistic quantifying the unpredictability of fluctuations in a time series used was the approximate entropy (ApEn) and was shown to have a Pearson's correlation of $R = 0.26$, $p < 0.05$, indicating that the higher the AFR, the less organized the *RR* series. In our study, the effect the regularity of the *RR* series has in modelling AFR was further evaluated in the ME′ model showing a significant effect ($\beta'_3 = 0.105$, $p < 0.05$). Previous studies have shown that the *RR* irregularity during AF change in response to changes in autonomic tone induced by drugs (Platonov *et al* 2012, Corino *et al* 2015, Cygankiewicz *et al* 2015) and tilt-test (Patel *et al* 2018). However, it should be noted that increased *RR* irregularity may also be a direct effect of changes in atrial electrical activity as quantified by an increased AFR or variations in the atrioventricular node conduction (Plappert *et al* 2021). Out of the three HRV parameters considered, only SampEn was correlated with average AFR and had significant effect on AFR when considering the ME model. However, SampEn alone does not convey as much information on the *RR* characteristics as when combined with the mean *RR* and RMSSD. A comparison between the ME′ model and a model excluding the mean *RR* and RMSSD showed that the full model had a better fit to the data ($R^2 = 0.56$, AIC = 4298 versus $R^2 = 0.51$, AIC = 4408).

Out of the 99 patients included, 19 (19%) had a previous ablation. Evidence of negative correlation between the percentage of fibrotic tissue in the left atria with the fibrillatory frequency have been reported (Swartz *et al* 2009). However, our study suggests that the number of ablations has a positive significant effect on AFR ($\beta'_5 = 0.168$, $p < 0.05$) with patients having gone through a higher number of ablations, having higher AFR.

Though further investigation with mapping and electrogram recordings is needed, this result suggests that creating lesions in the atria reduces macro-reentrant pathways but at the same time, promotes micro-reentrant circuits and/or faster, smaller rotors which would increase the fibrillatory rate of the atria.

Trying to understand AF behaviour, the link between AF episode duration and AFR had been previously studied showing a positive correlation between them ($R = 0.53$, $p < 0.05$) (Bollmann *et al* 1999). The study showed that having a higher AFR at the start of the AF episode could predict longer episodes. However, this study was conducted in a small dataset with only 31 episodes from 11 paroxysmal AF patients and the correlation was describing the whole database without explicitly considering intra- and inter-patient effects. The results of the present study confirm Bollmann's results as the episode duration had a significant effect on the AFR in the ME′ model ($\beta'_7 = 1.182 \times 10^{-5}$, $p < 0.05$). Finding of longer episodes of AF having higher AFR could be explained by an increase of sympathetic drive with longer duration of arrhythmia (Carnagarin *et al* 2019). The Reveal LINQ detects AF episodes of 2 min duration and longer, and hence AF episodes of 30 s to 2 min remain undetected. However, 'Duration' is still considered a necessary variable in the model due to the large spread of episode durations on the data: with the minimum duration being the detection threshold, i.e. 2 min, and the maximum duration spanning 62.7 d. With these large duration ranges, even if the episodes are evaluated in bins of 2 min, the effect of long versus short durations on AFR can be evaluated accurately.

In several studies, circadian dynamics of AFR were observed in patients using Holter monitoring (Bollmann *et al* 2000, Cosson *et al* 2000, Meurling *et al* 2001). In these studies, AFR showed a decrease at night and an increase during the morning hours, with a peak during the afternoon. In one of those studies, two different sets of patients were identified: one which showed an increase (minority) while the other showed a decrease (majority) in nocturnal AFR (Bollmann *et al* 2000). However, the insight in circadian behaviour of atrial electrophysiological characteristics during AF was constrained to 24 h long Holter registrations and limited datasets of up to 30 patients. The present study is based on a larger study population (99 patients) and longer monitoring periods (0.2−24.3 months), and no significant fixed effect of the onset time was observed when modelling the AFR. Circadian variation in the AFR is caused by autonomic modulation in the atrial electrical activity and could potentially be used to guide clinical strategies such as time of the day medication should be administered, or which patient would benefit the most from a catheter ablation procedure.

Currently, there is still uncertainty about the optimal selection for catheter ablation and overall, the challenges to define clear patients' phenotypes for appropriate AF management are still prominent (Karamichalakis *et al* 2015, Heijman *et al* 2018). Our study suggests that continuous assessment of AFR has the potential to estimate the impact of therapies and therefore, to help the stratification of patients towards AF ablation especially when it can help the physician decide whether or not to recommend ablation therapy and persist in drug treatment.

To assess the importance of including patient specific dependencies on *RR* series characteristics in the model, the results were compared to an ME model that only considered $\boldsymbol{b}_0$. This model had a better performance compared to the *FE* model ($R^2 = 0.37$; $AIC = 4727$ versus $R^2 = 0.05$; $AIC = 5699$) but had a worse fit to the data than the ME model ($R^2 = 0.49$; $AIC = 4424$). This shows that the patients still have a high heterogeneity not being addressed by the model but some of it can be found in their *RR* characteristics.

Detailed results for the estimated random effects of the ME' model can be found in the supplementary material. For most patients, the random effects coefficients were non-significant. However, for a subset of patients, the HR variables had negative significant effect on the AFR (mean *RR*: 6, RMSSD: 5, and SampEn: 3 patients) while for another subset, they had a positive significant effect (mean *RR*: 8, RMSSD: 6, and SampEn: 8 patients). The rest of the random effect coefficients had a negative significant effect on the AFR of a subset of patients (Time: 5, number of Ablations: 2, Days from Implant: 5, and Duration: 1 patient) while for another subset of patients, they had a positive significant effect (Time: 3, number of Ablations: 2, Days from Implant: 4, and Duration: 4 patients). For the rest of the patients, there were no significant random effect coefficients. This shows the heterogeneity in the dataset and proves the rationale of needing ME models to analyze such cohort.

This retrospective study combining 2 different cohorts with limited clinical baseline data, is selected from a patient population implanted with the Reveal LINQ based on clinical indications including suspected AF, AF ablation monitoring or AF management. Although this unique database offers the advantage of long monitoring periods and a complete monitorization of patients suffering AF, some limitations should be noted. The patient population included in the study is relatively young (57 ± 12 years) compared to the general AF population and with a low degree of cardiovascular risk. Due to the retrospective nature of the study, the medication administered to each patient during the monitoring period and the ablation technique in those patients with a previous failed ablation were not available. In a similar manner, the gender of the patient was not available and its influence on AFR could not be assessed. In any case, possible influence of medication, scar tissue from previous ablations and gender on AFR is modelled as a patient specific random effect. Furthermore, due to the limited memory of the device, ECG data was only stored for a subset of the detected episodes; 57 840 episodes were detected by the device out of which ECG data from 3739 (6.5%) were stored. The number of episodes

detected but not stored is not only linked to the number of episodes suffered by the patient but also to the frequency of visits to the hospital as the data was downloaded and saved each time the patient had a check-up. Overall, the patients had a median (min-max) of 130 (1–4564) episodes detected pre-ablation out of which 43.4 (1.9–100)% were stored. Post-ablation, the device detected 1 (0–4245) episodes out of which 60.2 (2.9–100)% were stored. The aim of this study involves analyzing the relationship between AFR and HRV features during the initial 2 min of the episodes while also accounting for various confounding factors. However, these first 2 min may not be representative of the whole episode; results from a previous study suggest that AFR may accelerate during the first 3–4 h (Platonov *et al* 2012). Therefore, the relationship between AFR and the HRV features might be different in other instances of the episode.

The extraction of atrial activity has been a difficult problem since the atrial and ventricular activities overlap spectrally and there is no uniform standard. There are two main approaches that exploit the property that atrial and ventricular activities arise from different bioelectrical sources: principal component analysis (PCA) (Raine *et al* 2004) and independent component analysis (ICA) (Rieta *et al* 2004). However, these approaches derive a global atrial signal with contributions from all the leads while the QRST cancellation technique used in this study (Stridh and Sörnmo 2001), extracts the atrial signal in a specific lead and strives at not modifying the original f-wave morphology. Despite their differences, in a comparative study between these three algorithms applied to the same surface ECG recordings, the dominant rate of the atrial signals extracted by each of the algorithms was within 1Hz (Langley *et al* 2002). The performance of the QRST cancellation technique was explored in both AF simulated signals and ECG data with AF and it was showed to be well-suited for atrial activation extraction (Stridh and Sörnmo 2001). In addition, there have been direct comparisons between endocardial signals and surface ECG signals subjected to the QRST cancellation technique used, summarized in (Bollmann *et al* 2006). The feasibility of extracting atrial activation from ICM data has been previously explored (Platonov *et al* 2012) where patients with paroxysmal AF received an implantable loop recorder (same one used in this study) and the AFR was extracted from episodes longer than 1 h also using the AFR tracker software provided by CardioLund. Conversely, in this study AFR was extracted from any episode longer than 2 min detected by the ICM and from both paroxysmal and persistent patients. The harmonic f-wave model used for AFR estimation was originally developed for surface ECG, and the characteristics of the f-waves in the ECG recorded by the ICM may differ from these since the electrodes are placed next to the apex of the heart (with V2-V3 electrode orientation). However, our results indicate that the model fit was sufficient in most cases; 2908 of the 3739 detected AF episodes in our 99-patient cohort had sufficient signal quality to be analysed.

5. Conclusion

Fixed and mixed effects modelling approaches were used to investigate the effect of changes in *RR* series characteristics corrected for episode onset and duration, previous ablations, and onset date, on variations in AFR in a study population of 99 patients monitored for 9.2 (0.2–24.3) months as median (min-max). The ME modelling approach was shown to be superior to the FE modelling approach due to the heterogeneity of the patient population and the presence of confounding factors. The fixed effects extracted from the ME′ model showed that AFR is slightly higher in episodes with less organized *RR* series and of longer duration and is affected by catheter ablations. The use of ME models combined with long term monitoring of patients offers the chance of continuously estimating the AFR from *RR* series and episode-based characteristic and will lead to a more detailed characterization and a better understanding of the patients' condition which could potentially aid the clinicians in their decision-making process. However, the results obtained point out the difficulties and unreliability of estimating AFR using such simple regression models. Further research with larger datasets that would allow for more complex models is warranted.

Data availability statement

The data cannot be made publicly available upon publication because no suitable repository exists for hosting data in this field of study. The data that support the findings of this study are available upon reasonable request from the authors.

Funding

Ethical statement

Our study was of retrospective nature and while we use data from clinical trials, the study itself did not partake in the trials. The data was collected from different participating institutions stated in https://clinicaltrials.gov/ct2/show/NCT01965899. The patients provided written informed consent, and the study protocols were reviewed and approved by the Human Research Ethics Committee of each participating institution in accordance with the Declaration of Helsinki.

References

Akaike H 1974 A new look at the statistical model identification *IEEE Trans. Autom. Control* **19** 716–23

Alcaraz R and José J R 2007 Wavelet bidomain regularity analysis to predict spontaneous termination of atrial fibrillation *Annual Int. Conf. of the IEEE Engineering in Medicine and Biology - Proc.* pp 1838–41

Altman D G and Bland J M 1983 Measurement in medicine: the analysis of method comparison studies *Statistician* **32** 307

Belsley D 1991 A guide to using the collinearity diagnostics computer science in economics and management *Comput. Sci. Econ. Manag. Volume.* **4** 33–50

Bollmann A *et al* 2006 Analysis of surface electrocardiograms in atrial fibrillation: techniques, research, and clinical applications *Europace* **8** 911–26

Bollmann A, Daniela H, Reiko S, Martin S, Leif S, Bertil Olsson S, Daniela P, Jochen M, Christoph G and Klein H U 2003 Echocardiographic and electrocardiographic predictors for atrial fibrillation recurrence following cardioversion *J. Cardiovascular Electrophysiol.* **14** S162–5

Bollmann A, Sonne K, Esperer H D, Toepffer I, Langberg J J and Klein H U 1999 Non-invasive assessment of fibrillatory activity in patients with paroxysmal and persistent atrial fibrillation using the holter ECG *Cardiovascular Res.* **44** 60–6

Bollmann A, Sonne K, Esperer H D, Toepffer I and Klein H U 2000 Circadian variations in atrial fibrillatory frequency in persistent human atrial fibrillation *PACE - Pacing Clin. Electrophysiol.* **23** 1867–71

Bollmann A, Tveit A, Daniela H, Stridh M, Sörnmo L, Pål S and Bertil Olsson S 2008 Fibrillatory rate response to candesartan in persistent atrial fibrillation *Europace* **10** 1138–44

Bou Ezzeddine H, Vachulova A, Svetlosak M, Urban L, Hlivak P, Margitfalvi P, Bernat V, Gladisova K, Sasov M and Hatala R 2015 Occurrence of symptoms after catheter ablation of atrial fibrillation *Bratislava Med. J.* **116** 461–4

Carnagarin R, Kiuchi M G, Ho J K, Matthews V B and Schlaich M P 2019 Sympathetic nervous system activation and its modulation: role in atrial fibrillation *Front. Neurosci.* **13** 1–16

Corino V D A, Ulimoen S R, Enger S, Mainardi L T, Tveit A and Platonov P G 2015 Rate-control drugs affect variability and irregularity measures of RR intervals in patients with permanent atrial fibrillation *J. Cardiovascular Electrophysiol.* **26** 137–41

Corino V D A, Cygankiewicz I, Mainardi L T, Stridh M, Vasquez R, De Luna A B, Holmqvist F, Zareba W and Platonov P G 2013 Association between atrial fibrillatory rate and heart rate variability in patients with atrial fibrillation and congestive heart failure *Ann. Noninvasive Electrocardiology* **18** 41–50

Corino V D A, Mainardi L T, Bollmann A, Husser D, Stridh M and Sörnmo L 2007 A Gaussian mixture model for time-frequency analysis of atrial fibrillation electrocardiograms *Annual Int. Conf. of the IEEE Engineering in Medicine and Biology - Proc.* pp 271–4

Cosson S, Maison-Blanche P, Bertil Olsson S, Leenhardt A, Badilini F and Coumel P 2000 Circadian modulation of atrial cycle length in human chronic permanent atrial fibrillation: a noninvasive assessment using long-term surface ECG *Ann. Noninvasive Electrocardiology* **5** 270–8

Cygankiewicz I, Corino V, Vazquez R, Bayes-Genis A, Mainardi L, Zareba W, Bayes de Luna A and Platonov P G 2015 Reduced irregularity of ventricular response during atrial fibrillation and long-term outcome in patients with heart failure *Am. J. Cardiol.* **116** 1071–5

Etgen T, Manfred Hochreiter, Markus M and Thomas F 2013 Insertable cardiac event recorder in detection of atrial fibrillation after cryptogenic stroke: an audit report *Stroke* **44** 2007–9

Heijman J, Guichard J-B, Dobrev D and Nattel S 2018 Translational challenges in atrial fibrillation *Circ. Res.* **122** 752–73

Henriksson M, Andrius P, Vaidotas M, Frida S and Leif S 2018 Model-based assessment of f-wave signal quality in patients with atrial fibrillation *IEEE Trans. Biomed. Eng.* **65** 2600–11

Hindricks G *et al* 2021 2020 ESC guidelines for the diagnosis and management of atrial fibrillation developed in collaboration with the european association for cardio-thoracic surgery (EACTS) *Eur. Heart J.* **42** 373–498

Hindricks G, Evgueny P, Lubos U, Milos T, Karl Heinz K, Dmitry L, Guido R and Pürerfellner H 2010 Performance of a new leadless implantable cardiac monitor in detecting and quantifying atrial fibrillation results of the XPECT trial *Circ.: Arrhythmia Electrophysiol.* **3** 141–7

Kapa S *et al* 2013 Assessing arrhythmia burden after catheter ablation of atrial fibrillation using an implantable loop recorder: the abacus study *J. Cardiovascular Electrophysiol.* **24** 875–81

Karamichalakis N, Konstantinos P L, Vlachos K, Georgopoulos S, Bakalakos A, Efremidis M and Sideris A 2015 Managing atrial fibrillation in the very elderly patient: challenges and solutions *Vascular Health Risk Manage.* **11** 555–62

Langley P, Stridh M, Rieta J J, Sörnmo L, Millet-Roig J and Murray A 2002 Comparison of atrial rhythm extraction techniques for the estimation of the main atrial frequency from the 12-lead electrocardiogram in atrial fibrillation *Comput. Cardiol.* **29** 29–32

Lee R and Mittal S 2018 Utility and limitations of long-term monitoring of atrial fibrillation using an implantable loop recorder *Heart Rhythm* **15** 287–95

Meurling C J, Waktare J E P, Holmqvist F, Hedman A, Camm A J, Olsson S B and Malik M 2001 Diurnal variations of the dominant cycle length of chronic atrial fibrillation *Am. J. Physiol. - Heart Circulatory Physiol.* **280** 401–6

Murray C, Wang H, Naghavi M, Allen C, Barber R, Bhutta Z and Carter D 2016 Global, regional, and national life expectancy, all-cause mortality, and cause-specific mortality for 249 causes of death, 1980–2015: a systematic analysis for the global burden of disease study 2015 *Lancet* **388** 1459–544

Patel H C, Hayward C, Wardle A J, Middleton L, Lyon A R, Mario C D, Salukhe T V, Sutton R and Rosen S D 2018 The effect of head-up tilt upon markers of heart rate variability in patients with atrial fibrillation *Ann. Noninvasive Electrocardiology* **23** 1–11

Plappert F, Wallman M, Platonov P and Sandberg F 2021 Changes in RR series characteristics during atrial fibrillation: an AV node simulation study *In 2021 Comput. Cardiol. (CinC)* **48** 1–4

Platonov P G, Cygankiewicz I, Stridh M, Holmqvist F, Vazquez R, Bayes-Genis A, McNitt S, Zareba W and de Luna A B 2012 Low atrial fibrillatory rate is associated with poor outcome in patients with mild to moderate heart failure *Circulation. Arrhythmia Electrophysiol.* **5** 77–83

Platonov P G, Stridh M, de Melis M, Urban L, Carlson J, Corbucci G and Holmqvist F 2012 Analysis of atrial fibrillatory rate during spontaneous episodes of atrial fibrillation in humans using implantable loop recorder electrocardiogram *J. Electrocardiol.* **45** 723–6

Platonov P G, Valentina D A C, Seifert M, Holmqvist F and Sörnmo L 2014 Atrial fibrillatory rate in the clinical context: natural course and prediction of intervention outcome *Europace* **16** iv110–9

Raine D, Langley P, Murray A, Dunuwille A and Bourke J P 2004 Surface atrial frequency analysis in patients with atrial fibrillation: a tool for evaluating the effects of intervention *J. Cardiovascular Electrophysiol.* **15** 1021–6

Richman J S and Moorman J R 2000 Physiological time-series analysis using approximate entropy and sample entropy maturity in premature infants physiological time-series analysis using approximate entropy and sample entropy *Am. J. Physiol. Heart Circulatory Physiology* **278** H2039–49

Rieta J J, Castells F, Sánchez C, Zarzoso V and Millet J 2004 Atrial activity extraction for atrial fibrillation analysis using blind source separation *IEEE Trans. Bio-Med. Eng.* **51** 1176–86

Rottner L *et al* 2020 Catheter ablation of atrial fibrillation: state of the art and future perspectives.' *Cardiol. Ther.* **9** 45–58

Saglietto A, Ballatore A, Gaita F, Scaglione M, De Ponti R, Maria De Ferrari G and Anselmino M 2021 Comparative efficacy and safety of different catheter ablation strategies for persistent atrial fibrillation: a network meta-analysis of randomized clinical trials *Eur. Heart J. Quality Care Clin. Outcomes* **8** 619–29

Sandberg F, Bollmann A, Husser D, Stridh M and Sörnmo L 2010 Circadian variation in dominant atrial fibrillation frequency in persistent atrial fibrillation *Physiol. Meas.* **31** 531–42

Sanders P, Pürerfellner H, Pokushalov E, Sarkar S, Di Bacco M, Maus B and Dekker L R C 2016 Performance of a new atrial fibrillation detection algorithm in a miniaturized insertable cardiac monitor: results from the reveal LINQ usability study *Heart Rhythm* **13** 1425–30

Stridh M and Sörnmo L 2001 Spatiotemporal QRST cancellation techniques for analysis of atrial fibrillation *IEEE Trans Biomed Eng.* **48** 105–11

Stroup W W 2013 *Generalized Linear Mixed Models: Modern Concepts, Methods and Applications by Walter W. Stroup* (Boca Raton, FL: CRC Press) (*Texts in Statistical Science Series*) vol 81 (https://doi.org/10.1111/insr.12042_24)

Swartz M F *et al* 2009 Left versus right atrial difference in dominant frequency, K+ channel transcripts, and fibrosis in patients developing atrial fibrillation after cardiac surgery *Heart Rhythm* **6** 1415–22

Verma A, Champagne J, Sapp J, Essebag V, Novak P, Skanes A, Morillo C A, Khaykin Y and Birnie D 2013 Discerning the incidence of symptomatic and asymptomatic episodes of atrial fibrillation before and after catheter ablation (DISCERN AF): a prospective, multicenter study *JAMA Internal Med.* **173** 149–56

Wright S 1921 Correlation and causation *J. Agric. Res.* **20** 557–85

Zeng T, Li Y and Yu J 2014 Deviance information criterion for comparing var models *Adv. Econometrics* **33** 615–37